

Application of (Kohn-Sham) Density-Functional Theory to Real Materials

Luca M. Ghiringhelli

Abstract

Hohenberg and Kohn proved the existence and uniqueness of a functional of the electron density, whose minimization yields the ground-state density $n(r)$ of a bound system of N interacting electrons in some external potential $v(r)$. The exact expression of the universal density functional is however elusive. In this chapter, I describe the several attempts made for designing an approximation to the density functional that gave accurate results for “real materials” (molecules, clusters, and extended materials). All discussed approximations originate from the Kohn-Sham approach, a particular (but almost universally adopted) formulation of the density-functional theory, in which the variational problem of the N interacting electrons is recast into a set of N one-particle equations where each electron acts in the mean field generated by all the other electrons.

1 Introduction

Density-functional theory provides the *exact* ground state density ($n(\mathbf{r})$) and wave function for a system of N electrons under a given external potential (e.g. as given by positively charged nuclei, in a given configuration). This is possible thanks to the universal functional, whose existence and uniqueness was demonstrated by Hohenberg and Kohn [1]. Unfortunately, although Levi [2] and Lieb [3] showed a formal way to construct the universal functional, as of today we do not know its analytic expression (see chapter by Delle Site for a detailed formal introduction of DFT). This limitation did not stop the immense success and diffusion of the theory, due to the

Luca M. Ghiringhelli
Fritz-Haber-Institut, Faradayweg 4–6, D-14195 Berlin-Dahlem, Germany
e-mail: ghiringhelli@fhi-berlin.mpg.de

fact that Kohn and Sham [4] were able to recast the variational problem of the N interacting electrons into a set of N one-particle equations, where each electron acts in the mean field generated by all the other electrons. This is not the only way to tackle the DFT problem, but by far the most followed one (see chapters by Trickey and by Delle Site for alternative approaches). With the Kohn-Sham formulation, the kinetic energy functional (of non-interacting particles) becomes trivial and the focus is shifted to the exchange and correlation (xc) functional ($E_{xc}[n(\mathbf{r})]$), which in turn is universal, but unknown. Several chapters in this book deal with the Kohn-Sham (KS) formulation of DFT, in particular for computational implementations and applications see the chapters of Tzanov and Tuckerman, Watermann *et al.*, and von Lilienfeld. In this chapter I will review the most successful *approximate* xc functional that were proposed since the introduction of KS-DFT, highlighting strong and weak points of each of them.

Knowing and predicting properties of materials in their geometric global minimum at a given composition is not enough for knowing how they behave in realistic conditions. Among the “realistic conditions”, the most important is temperature. Prediction of the behavior of a system at positive temperature requires the appropriate sampling of the canonical ensemble. Besides temperature, a real material on Earth is necessarily exposed to the effect of (possibly humid) air or other artificial mixtures of reactive gases, which will modify its surfaces from the global minimum (corresponding to ultra-high vacuum conditions, at low temperature).

In the last two sections, I summarize how accurate and affordable DFT calculations can be performed in order to predict the behavior of materials at the mentioned realistic conditions.

2 Successes and Failures of Local and Semilocal Functionals

The historically first and simplest approximation for $E_{xc}[n(\mathbf{r})]$ is the so-called local-density approximation (LDA),

$$E_{xc}^{\text{LDA}} \equiv \int e_{xc}(n(\mathbf{r})) n(\mathbf{r}) d\mathbf{r} \quad (1)$$

where $e_{xc}(n)$ is the exchange-correlation energy per particle of a uniform electron gas of density n [4]. It is expressed as the sum of an exchange and correlation part. The former (in atomic units) is elementary: $e_x = -0.458/r_s$ where the Wigner-Seitz radius (r_s) is the radius of a sphere containing one electron ($n^{-1} = 4\pi/3r_s^3$). The correlation part was first estimated by E. P. Wigner [5]: $e_c(n) = -0.44/(r_s + 7.8)$. Later, analytic expressions at high and at low density (corresponding to infinitely weak and strong correlations) were derived, and in the intermediate regime highly accurate values were evaluated via Monte Carlo sampling [6].

LDA, albeit exact by construction for a uniform electron gas, was expected to be useful only for densities varying slowly on the scales of the local Fermi wavelength

and Thomas-Fermi wavelength. In atomic systems these conditions are rarely well satisfied and very often seriously violated. Nevertheless the LDA has been found to give extremely useful results for most applications. This has been at least partly rationalized by the observation that the LDA satisfies a sum rule which expresses the normalization of the exchange-correlation hole: Given that an electron is at \mathbf{r} , the conditional electron density $n(\mathbf{r}; \mathbf{r}')$ of the other electrons is depleted near \mathbf{r} , in comparison with the average density, by the hole distribution $n_h(\mathbf{r}'; \mathbf{r})$ which integrates to unity.

LDA's error for the exchange energy [7] is typically of the order of 10%, while the correlation energy (normally much smaller) is in general overestimated by up to a factor of two. Thus, the two errors are typically found to partially cancel. Practice has shown that the LDA gives ionization energies of atoms, dissociation energies of molecules and cohesive energies of solids with an accuracy of typically 10% – 20%. Nonetheless, bond lengths and thus the geometries of molecules and solids predicted by the LDA are typically with a remarkable (and somewhat unexpected) accuracy of 1%.

A new level of complexity for deriving approximate xc functionals is the so called Generalized-gradient approximation (GGA) to the xc functional [9], where the xc energy also depends on the density gradient at a given point. Differently from LDA, a xc functional constructed within the GGA is not unique. Successful, hence popular, examples of GGA functionals are the Perdew-Burke-Ernzerhof (PBE) [10] and revised PBE, revPBE [11], which are fit to the exact exchange energy of rare-gas atoms. GGA functionals partially correct the LDA for inhomogeneous electron densities. Molecular atomization energies are significantly improved. With PBE, lattice constants of solids are (typically) overestimated within 2% from experiment. It underestimates solid cohesive energies and bulk moduli by 10% – 20%. For molecules, the underestimation of intermolecular interaction energies is more severe (60%). GGA functionals do not mend the self-interaction error.

An outstanding failure of LDA and GGA xc functionals has been their inability to provide good estimates of the fundamental gaps of semiconductors and insulators, a crucial quantity for much materials research, such as impurity levels in doped semiconductors [12]. Calling I the ionization potential and A the electron affinity, the fundamental (or transport) gap is $I - A$ (note that this quantity is a ground-state property of an electronic system). It is well established that the KS gap, i.e., the difference between the energies of the KS highest-occupied molecular orbital (HOMO) and of the lowest-unoccupied molecular orbital (LUMO) in a molecule/cluster (valence band maximum and conduction band minimum in a solid), does not equal this $I - A$, even with the exact xc functional [13, 14]. Calculations suggest that the KS gap is typically substantially smaller (by about 50%) than the fundamental gap for semiconducting solids [15]. The LDA and GGA approximations yield accurate KS gaps, but it is the fundamental gap that is of real interest. In principle, $I - A$ can be found by adding and subtracting electrons from a large atomic cluster with the symmetry of the bulk material. Unfortunately, in LDA or GGA, this gap, found by total energy differences, incorrectly collapses to the KS gap, because these approximations wrongly allow electrons to completely delocalize over insulating solids. This property is also related

to the fact that such approximations lack a derivative discontinuity that prevents this over delocalization [14].

Another crucial deficiency of LDA and GGA approximations is their incorrect accounting of long-range correlations, in particular van-der-Waals (vdW) interactions (see also in this book the chapters by Malet *et al.* for strongly interacting electrons, and by Watermann *et al.* for vdW).

3 Mending the Self-Interaction Error: Hybrid Functionals

In the early 1990s, hybrid functionals were introduced by Becke [24], by treating the exchange term as orbital-dependent, via generalized KS theory [26]. In practice, a fraction (typically 20%) of GGA exchange is replaced with Hartree-Fock (HF) exchange. This approach led to the ubiquitous B3LYP [25], the most popular approximation in use in theoretical chemistry today. Since in HF theory the self-interaction error is absent, hybrid xc functionals show typically a much smaller self-interaction error. This implies that, compared to LDA and GGA, hybrid functionals yield more accurate fundamental gaps for semiconductor materials. A recent functional, called HSE [27] not only mixes in some HF, but also performs a range-separation. Based on exact theorems of Savin [28] the short-range part of the HF exchange is treated exactly, while the long-range contribution is treated by approximate DFT. The resulting functional, used to calculate gaps in the generalized scheme, appears to work accurately for a large variety of moderate-gap semiconductors [27]. It yields accurate fundamental gaps when excitonic effects are negligible, and is closer to optical gaps when they are not [29, 30], provided the range-separation length is appropriately optimized.

4 Rationalizing the Performance: Data Sets

Before describing how the problems of LDA and GGA xc functionals were addressed and largely overcome, it is worthwhile to present a relatively recently introduced set of criteria for evaluating the performance of old and new xc functionals. In the past twenty years benchmark data sets of ground states of molecules and molecular processes have been created in quantum chemistry and their impact is steadily growing. Their practical utility and critical value is to offer a set of criteria for objectively evaluating the performance of various electronic-structure methods, both in the DFT and WFT communities. In such test sets, the reported quantities are evaluated with the high-level (post-Hartree-Fock) first principle quantum chemistry methods available today, typically “coupled-cluster theory with single, double, and perturbative triple substitutions”, CCSD(T) [16]. The great merit of the data sets based on reliable high-level electronic-structure theory calculations is to disconnect theory from experiments. While this may sound rather as a limit, as experiments can potentially

be extremely accurate and guarantee an unquestionable description of reality, the choice of a theoretical method as benchmark, provides the unique opportunity to directly compare the quantities that the tested method yields — namely the energy of a molecule or molecular complex — not a derived property that can be measured experimentally. In particular the comparison can be based on *exactly* the same molecular geometry and immune to complicated relativistic and electronic-vibrational coupling effects, making the comparison simple and well-defined.

Examples of such data sets are: the W4-08 set [18] where atomization energies of 99 covalent molecules are listed; the S22 set [19] containing 22 bio-oriented weakly-bound molecular complexes of different size and bonding type (seven of hydrogen bonding, eight of dispersion bonding, and seven of mixed nature); the more comprehensive S66 set [20], containing 66 weakly bound molecular complexes; HTBH38 [21] containing the forward and inverse barrier heights of 19 hydrogen-transfer reactions, and NHTBH38 [22] with 19 reactions involving heavy atom transfers, nucleophilic substitutions, association, and unimolecular processes.[17] Recently, a thorough benchmark data set GMTKN30 was proposed [23], which includes 30 subsets collected from the literature, covering a large cross section of chemically relevant properties of main-group molecules.

Figures of merit that are cited when testing an electronic-structure method vs a data set are the mean absolute relative error (MARE), the mean error (ME), the mean absolute error (MAE), the maximum absolute relative error (MaxARE), and the maximum absolute error (MaxAE).

As much as data sets for molecular ground states and processes are becoming more and more well assessed, at present reference data sets for an important class of systems, namely crystalline solids, are missing. The main reason of this lack is the impracticality of calculations with periodic boundary conditions (pbc) with a method like CCSD(T). In particular for complex (transition) metal systems, the accuracy of CCSD(T) is not yet fully verified. A data set on crystalline solids is however highly needed in computational materials science, as recently the improvement of computer power and efficiency of algorithms for the evaluation of the electronic structure of a given system (material) and for the sampling of its potential energy surface, put computational materials science in the position of scanning large amounts of different materials searching for optimized desirable properties. We may very interested to search for new efficient functional materials for, e.g. photovoltaics, heterogenous catalysis, and thermoelectrics. A prerequisite for this search to be successful is to require a controllable accuracy of the electronic-structure methods used for performing the search.

5 Improving the Description of Weak Interactions I: The Random Phase Approximation (RPA) and Beyond

Electron correlations as described by xc functionals introduced so far, are of (semi-) local nature (in practice, an electron “feels” other electrons only in its vicinity), while

van-der-Waals dispersion energy arises from the correlated motion of electrons often distant from each other; these correlations must be described by many-body quantum mechanics. While generally weaker compared to covalent bonds, vdW forces are crucial to properly describe, e.g. the so-called physisorption of organic molecules on inorganic and organic surfaces. Interestingly, they play a noticeable role even for chemisorption when strong chemical bonds are formed between docking groups of a molecule and the substrate (e.g., for self-assembled monolayers [SAMs] bonded to gold by thiolates [34]). Van-der-Waals interactions are found to contribute substantially also to the cohesion energy of bulk noble metals [35].

An exact route toward the description of vdW interactions in DFT is provided by the adiabatic connection fluctuation-dissipation (ACFD) theorem [36, 37]. The ground-state total energy of an interacting many-body Hamiltonian can formally be obtained via the adiabatic-connection (AC) technique, in which a continuous set of coupling-strength (λ)-dependent Hamiltonians is introduced that “connect” a reference Hamiltonian with the target many-body Hamiltonian. In KS-DFT, the adiabatic switching-on of the Coulomb interaction between electrons is done along a path that is chosen such that the electron density is kept fixed at its physical value. In this way an exact expression of the xc functional is recast in terms of density-density correlations (fluctuations). The density - density correlations are linked to the response properties (dissipation) of the system through the zero-temperature “fluctuation-dissipation” theorem (FDT). The FDT is a powerful technique in statistical physics. It states that the response of a system at thermodynamic equilibrium to a small external perturbation is the same as its response to the spontaneous internal fluctuations in the absence of the perturbation. Full ACFD-DFT calculations, however, are unfeasible, hence approximations must be employed. In this context, the “random-phase approximation” (RPA) is a particularly simple approximation of the response function.

The RPA for electron correlation (cRPA), combined with the exact HF treatment of exchange (hence, EX+cRPA) [31] has recently gained popularity. This method yields a remarkable performance for lattice constants (1.4%) and bulk moduli of solids (11%) [32]

The exact-exchange energy cancels the spurious self-interaction error present in the Hartree energy exactly (although the RPA correlation itself does contain some self-correlation and is non-zero for one-electron systems). The RPA correlation energy is fully non-local and includes long-range vdW interactions automatically and seamlessly. Moreover, dynamic electronic screening is taken into account by summing up a sequence of “ring” diagrams to infinite order, which makes RPA applicable to small-gap or metallic systems where finite-order many-body perturbation theories break down.

Although cRPA yields the correct C_6/R_{ij}^6 asymptotic behavior for a pair of well-separated finite systems [38] (R_{ij} is the distance between fragments i and j , and C_6 is the associated dispersion coefficient), it is not accurate for short-range correlations [39, 40]. In particular, it has been reported a systematic underestimation of binding energies and a failure to describe stretched radicals [41]. This has limited the applicability of the method until in recent times a systematic improvement has been achieved

by including renormalized single-excitation (rSE) corrections [42] (a concept borrowed from many-body perturbation theory), and second-order screened exchange, SOSEX, [43]. The method that employs EX for the exchange and cRPA+rSE+SOSEX for the correlations is called renormalized second order perturbation theory (rPT2) [43]. This method has been shown [41] to yield a remarkable accuracy for dissociation energy of dimers, vdW interactions (S22 set, see Fig. 1), reaction-barrier heights (HTBH3 and NHTBH3 sets), and good performance for atomization energies (G2-1 set), all the above benchmarked to CCSD(T) calculations.

RPA based methods are an area of active research. In particular, there is a great interest in developing schemes that offer a reduced computational cost, schemes that provide RPA-level forces and schemes that achieve self-consistency, in order to eliminate or at least greatly reduce the dependence on the input orbitals.

6 Improving the Description of Weak Interactions II: Long-Range Corrections to “Traditional” xc Functionals

Langreth et al. developed the vdW-DF functional over the last decade [45, 46, 47]. Like the RPA, it is based on the ACFD theorem. Characteristic for DFT calculations, the corresponding nonlocal correlation energy contribution is obtained from the electron density only. The local electron correlation is treated by LDA, while the exchange energy is described by the generalized gradient approximation (GGA) to the xc functional, specifically the revPBE [11] functional. The approach is very attractive, as it is derived from first principles and does not rely on empirical parameters or fitting. With recent implementations [48] its computational efficiency is comparable to that of standard DFT-GGA calculations. However, especially for intermolecular interactions, the performance of original vdW-DF is not spectacular [49]. The errors are around 20% – 30% for intermolecular energies and 0.3 – 0.4 Å for equilibrium distances. Furthermore, the accuracy for solids is not yet fully established. The improvement of vdW-DF is an active research field, and recent developments yield better accuracy by employing different exchange functionals than revPBE for the short range and/or by introducing parameters fitted to high-level quantum chemical binding energies. [50, 51].

In the chapter by Watermann *et al.* of this book an alternative approach to vdW-DF is described. Here, I focus on a different class of methods, i.e., adding the interatomic dispersion energy contributions to DFT total energies, typically only considering the leading-order $C_6R_{ij}^6$ term, with a cutoff at short distances. The pioneer of this class was the DFT-D approach, that has gained popularity after it was shown [33] that accurate results for intermolecular interactions can be achieved, and DFT-D can be connected to different functionals. It has shown good accuracy for intermolecular interactions (15% – 20% error for energies and 0.1 – 0.2 Å for equilibrium distances), and it has the same computational cost as the underlying DFT calculation. The main shortcoming of such DFT-D formulations is the high level of empiricism, requiring at least two fitting parameters for every element in the periodic table. Furthermore,

different possible hybridization/oxidation states of atoms in different chemical or geometrical environments were not accounted for.

Recently, several groups have proposed different solutions to these issues. In particular, Tkatchenko and Scheffler (TS) developed a method to obtain accurate dispersion coefficients and vdW radii directly from the ground-state molecular or condensed-matter electron density (DFT+vdW method) [44]. This approach starts from high-level quantum-chemistry calculations for free atoms, and then the changes that result from the interactions between atoms are obtained from the electron density of the polyatomic system. In practice, the tail correction is written as $C_6[n]R_{ij}^{-6}$, where each $C_6[n]$ is a functional of the DFT electron density n . There is a single parameter remaining in the DFT+vdW method, the vdW radius scaling. This parameter defines the linkage of the R_{ij}^6 vdW interaction and the DFT functional. The necessity of this parameter (the vdW radius) remains the main weakness of the approach. A strength of the DFT+vdW method and of the general DFT-D concept is that they can be easily coupled to different xc functionals. This approach shows remarkable accuracy for intermolecular interactions (8% error for energies and 0.1 Å for equilibrium distances), handles different hybridization states transparently, and has the same computational cost as the underlying DFT calculation. In the original formulation of Ref. [44], the method could not treat extended systems such as solids and (adsorption on) surfaces. Subsequently two other schemes for coping with (non-metallic) solids [54] and organic/inorganic interfaces [55] were introduced. In both cases the tail correction appears in the form $C_6[n]R_{ij}^{-6}$, but for the derivation of the $C_6[n]$ the non-local screening effect of the extended system is accounted for.

More recently, the TS method was further developed by including many-body contributions to the dispersion interactions [52, 53]. This is achieved by modeling the weakly interacting molecular fragments as a system of coupled quantum harmonic oscillators (QHO) within the random-phase approximation (RPA). The resulting many-body dispersion (MBD) method contains two types of energetic contributions that arise from beyond-pairwise (non-additive) interactions and electrodynamic response screening.

In Fig.1 a comparison of the relevant methods for the description of long-range correlations is shown.

7 Not so Universal: Parameters-Dependent Families of Functionals

As mentioned above, the first approximation to the xc functional was LDA, whose actual formulation is determined by properties of the uniform electron gas. No one disputes that DFT with LDA is non-empirical. However, even just the next step up in xc-functional sophistication, the GGA, has no unique form. Two fundamentally different approaches have been followed to design GGA (and higher-level) xc functionals. One school of thought, led by John Perdew [9, 10], uses exact conditions of quantum mechanics to derive the parameters for the (approximate) functionals. Following the

second kind of approach, one allows for one or few parameters to be fit to specific (real) systems. A typical example belonging to this approach is the LYP correlation of B3LYP [25]. Similar approximations are based on sound physical reasoning, indeed in some cases those fitted parameters could be also (later) derived from first principles [10]. It may be worth noting that if the fitting approach is followed, the resulting xc functional typically displays higher accuracy for systems similar to those fitted (often by a factor of two), but greater inaccuracies far away. For example, LYP correlation works very well as part of B3LYP in chemistry, but fails badly for bulk metals. The exact-conditions-based PBE approximation [10], in contrast, works fairly well for many features of extended (periodic) systems, but can be a factor of two or more worse than BLYP for dissociation energies. A simple example of a first-principles approach is given by the B3LYP approximation (and its materials counterpart, PBE0 [58]). The crucial choice for a hybrid functional, which mixes HF with GGA exchange, is the fraction of exact (HF) exchange, about 20% in B3LYP. This value was fixed once and for all in the definition of the functional. The amount of mixing can be rationally related to other aspects of atomization energies [58]. If authors adjust the amount of mixing to improve their results *for some system or property*, this is not first principles.

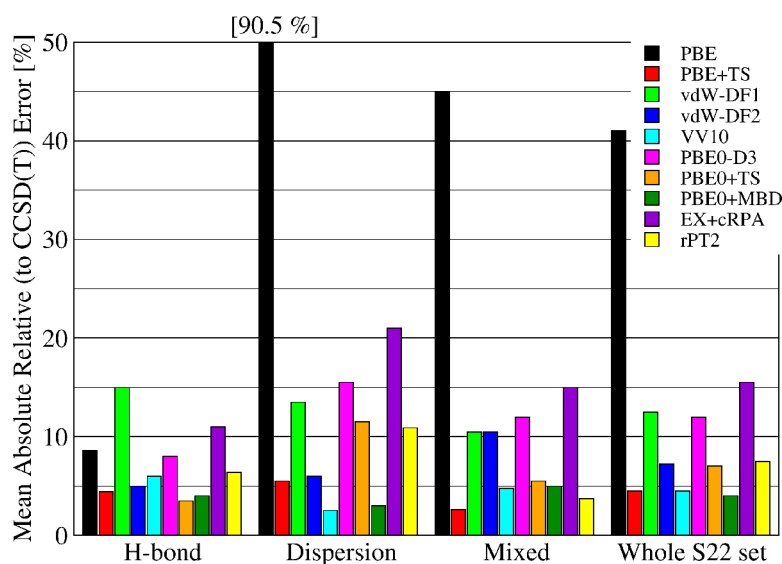


Fig. 1 Performance on the S22 [19] dataset of the relevant methods for the description of long-range correlations. The figure is created with data reported in Refs. [41, 49, 56]. The references for the reported functionals are: PBE [10], PBE+TS (PBE with Tkatchenko-Scheffler vdW correction) [44], vdW-DF1 and vdW-DF2 [57], VV10 [50], PBE0-D3 [33], PBE0+TS [44], PBE0+MBD (PBE0 with many-body dispersion correction) [53], EX+cRPA [31], rPT2 [43]. The mean absolute relative error for PBE in the “dispersion” subset of S22 far exceeds the range of the plot, as indicated by the number on the top of the bar.

A global optimization, i.e. valid for all systems may also use different criteria than optimizing to physical properties of a data set, for example, computational efficiency (of course, only possible if the computational cost associated with the functional is a function of one or more parameters). I focus on the HSE hybrid functional [61] as an example. This functional can be seen as signpost of a family of functionals, depending on (two) parameters. Perturbation theory [58] gives for the fraction of HF exchange $\alpha = 0.25$, but HSE belongs only in a generalized sense to the class of functionals treated in [58], the “adiabatic connection functionals”; in fact, only the short-range portion of the HSE functional is affected by the parameter α . In Ref. [61], α is fixed at 0.25, while the exchange screening parameter was tuned to $\omega = 0.11 \text{ bohr}^{-1}$ in order to minimize the error of enthalpies of formation, ionization potentials, and electron affinities of properly-selected group of data sets. Later, Chelikowsky and coworkers [60] treated both parameters (α, ω) as freely tunable, and found a slightly different pair ($\alpha = 0.313, \omega = 0.185 \text{ bohr}^{-1}$) that minimizes the error, defined with similar criteria as in [61]. Alternatively, the pair ($\alpha = 0.525, \omega = 0.408 \text{ bohr}^{-1}$) yields the same error as HSE06 ($\alpha = 0.25, \omega = 0.11 \text{ bohr}^{-1}$) but with a much shorter screening parameter, i.e., reduced computational cost.

An extreme example of the fitting approach is represented by the Minnesota xc functionals developed by Truhlar and coworkers, reviewed in Ref. [59]. These functionals adopt the same basic ingredients as the standard approximations, but optimize performance on a training set of energies by fitting up to several dozen parameters. These often produce more accurate results on systems close to those trained on and beyond, by employing functional forms that are more complex than those of the standard functionals, and challenge orthodoxy concerning the limitations of given levels of approximation [59]. Nonetheless, since these functionals contain no parameters adjusted to the system being calculated, they can be still considered as first-principles [8].

8 Positive Temperatures: DFT-Based Molecular Dynamics

The above analysis of the accuracy of approximate xc functional used in the practice of DFT, was based on dataset, i.e., on the (formation or interaction) energy and geometry of (meta)stable molecules, molecular complexes, and periodic structures. The assessment of such performances is a necessary step for a functional but is only preliminary before DFT can be applied to the description of realistic systems. The missing ingredient is the sampling of the potential energy surface (PES) at positive temperatures (canonical ensemble) and the possibility of changing the number of particles in the system (grand-canonical ensemble). In general the attention is shifted from the (local or global) minimization of the total energy (coulomb plus xc interactions) to the minimization of the properly defined free energy, i.e. analytically or statistically accounting for the entropy of the system at the given conditions. In this section, I briefly discuss the applications of a wide-spread technique to sample

the PES of a system at positive temperature ¹, while in the next section I describe a methodology that allows for the evaluation of the (meta)stability of materials in reactive environments at positive temperature.

Ab initio molecular dynamics (AIMD) simulations combine classical molecular dynamics simulations for the nuclei with electronic structure calculations. In classical molecular dynamics nuclei are treated as point particles and the Newtonian equations of motion are integrated numerically. The theoretical foundations for *ab initio* molecular dynamics were laid with the work of Ehrenfest [62] and Dirac [63] during the first half of the twentieth century. Dirac developed the theory of time-dependent self consistent field (SCF) equations for nuclear and electronic motion and Ehrenfest derived mixed classical-quantum mechanical (time-dependent electronic structure) equations. In 1985 it was the seminal article of Roberto Car and Michele Parrinello [64] which initiated the use and further development of *ab initio* molecular dynamics simulations. The authors intended to derive a new method which is able to “(i) compute ground-state electronic properties of large and/or disordered systems using state-of-the-art electronic structure calculations; (ii) perform AIMD simulations where the only assumptions are the validity of classical mechanics to describe ionic motion and the Born-Oppenheimer (BO) approximation to separate nuclear and electronic coordinates” [64]. For this purpose Car and Parrinello made use of the extended Lagrangian technique, previously invented to simulate systems under constant pressure [65, 66]. In practice, in BO-MD the electronic wave-function is optimized to its ground state at each time step, while in CPMD an approximated ground state is propagated by describing the wavefunction with auxiliary (fictitious) degrees of freedom.

For several years CPMD has dominated the field of AIMD due to its computational efficiency. Recently, however, more efficient algorithms for the scf convergence in DFT codes, in particular in connection with localized basis sets, made BO-MD more appealing, also considering that it generally allows for larger time steps than CPMD.

The time-span of AIMD is limited to few up to tens of ps (for a system of few tens of atoms), nonetheless reliable evaluations of several relevant quantities could be performed. For instance, order-to-disorder phase transitions in fluids [71, 72, 73] could be simulated, (self)diffusion and conductivity in liquids [74, 67], infrared (IR) spectra [68], NMR spectra [69], heat capacities [70]. CPMD proved to be well suited for describing several properties [75, 76] of the vapor phase [77], liquids [78, 79], mixtures, and solvent effects [80, 81], substitution [82] and redox [83] reactions in solution

A prerequisite for a meaningful sampling of the PES is that the accuracy of the adopted functional does not deteriorate far from geometrical local minima (forces are zero and their first derivatives wrt position are all positive). Some data sets take into account distorted geometries, in particular along a “reaction path” (examples are HTBH38 [21] and HTBH38 [22]), but more important is the overall accuracy, thus different data sets, for example benchmarked to (experimental) IR spectroscopy may

¹ The dynamics of the nuclei is treated at positive temperature, whereas the electronic wavefunction is considered at or near its ground state. Inclusion of non-adiabatic effects, i.e., loosely speaking, electronic excited levels are treated in this book in the chapter by Doltsinis. Since there is no widespread technique for beyond-BO MD, I do not mention further this class of methods

be more significant. For theoretical IR spectroscopy, time autocorrelation functions of the molecular dipole moment are averaged upon canonical sampling of the PES; hence both the accuracy of the functional and of the sampling method are stretched to their limit. I will not mention further the problem of having a proper canonical sampling of the PES, where also the dynamic correlations are preserved, except that it is an active area of research [84, 85].

Coupled to efficient techniques, such as thermodynamic integration, adiabatic switching [86], and metadynamics [87, 88], for the evaluation of difference in free-energies between two phases or in general two metastable states of one system, AIMD allowed for the accurate determination of the melting line of, e.g., diamond and nitrogen [89, 90], or the phase diagram of silica [91], accurate heat capacities and expansion coefficients of solids up to their melting line [70].

All the former works have one approximation in common: a system of few (tens or hundreds) atoms, typically periodically replicated via pbc, is used as a model for the behavior of a macroscopic, experimentally accessible system. In fact, in such studies, an evaluation of the size effect (i.e. the influence of the finiteness of the size of the system) on the the calculated thermodynamic values is typically performed. Recently, experiments on “single” (i.e. gas phase) molecules and clusters became possible and AIMD found a natural partner, where the assumption in comparing experiment to *ab initio* calculations are reduced to a minimum (yet not eliminated, e.g., the problem of ensuring thermodynamic equilibrium in gas phase experiments remains open). For example, positive-temperature IR spectra [92] and structural stability [93] of polipeptide alpha helices *in vacuo* were tested up to the unusual temperature of 700 K, in agreement with related experiments; the important role of the vdW interaction for the stability could then be singled out from the contribution given by the network of hydrogen bonds when the same molecules are in a (polar) solvent. Also, positive-temperature IR spectra of gold clusters [94], complexed with rare-gas atoms, could be compared to parallel experiments and thus it was possible to assign the structures of the isomers at different sizes.

9 Beyond the Perfect Specimen *in Vacuo*: *Ab Initio* Atomistic Thermodynamics

The behavior of a surface under ultra-high vacuum (UHV) conditions (10^{-13} – 10^{-9} atm) and low temperatures (e.g. room temperature and below) may be different from its behavior when exposed to a (reactive) gas at high pressures and temperatures: this is called the “pressure gap” [95]. In this respect, one of the main concerns in surface science has been the extrapolation from UHV conditions and single crystal substrates of surface science, to the high pressures and temperatures, and the often quite complex structures of industrial catalysts under reaction conditions. This deviation between the single crystals and “working” catalyst materials, has been coined the “material gap”. Because the native catalyst material may undergo sig-

nificant changes when under actual operating conditions, the material and pressure gaps are typically linked.

When a surface is in contact with a realistic environment, e.g. an atmosphere containing oxygen and water, atoms or molecules from the environment can adsorb on the surface and/or atoms from the surface can be released into the environment. What is typically called a stable surface structure is in fact a statistical average over adsorption and desorption processes.

For (near-)equilibrium system, a successful methodology for the prediction of stable and metastable structures at given environmental conditions is *ab initio* atomistic thermodynamics (AIAT), which, as the name suggests, combines atomistic (in practice, DFT) data with text-book thermodynamic concepts, in order to provide phase diagrams for the relative stability of structure, as function of the chemical potential of the involved species. In this sense, it is a multiscale approach, which enables the linking of the time and length (sub)nanoscale (i.e. around or less than nm and ns), accessible to *ab initio* calculations, to the meso- and macroscale accessible to experimental investigation. AIAT requires affordable additional computational cost (namely, calculation of phonons/vibrational spectra) on top of the usual local optimizations of structures. The key requirement is, however, to ensure that *all* relevant local minima of the PES of a given (open) system are found. If for controlled situations (e.g. defects in bulk, adsorption on surfaces) intuition and symmetry considerations may let convincingly *a priori* enumerate all the possible structures [96, 97], in other yet relevant cases (e.g., gas-phase and supported clusters in reactive environment) a thorough and unbiased global minimization should be carried out [98, 99, 100]. AIAT was initially [101, 102], but also recently [103], applied to the prediction of defects in bulk semiconductors, as function of the doping (captured by the Fermi-energy level). Later, it attracted widespread attention when applied to surface-oxide formation [96], stability of semiconductor surfaces [104], heterogeneous catalysis on metal-oxide surfaces [97] under “constrained equilibrium” conditions (the reactants do not react in the gas phase, but only with the aid of the catalytic surface, and the desorption of the product is the rate limiting step of the catalytic process).

The thermodynamic phase diagrams provided by AIAT may serve as a starting point for steady-state analyses where kinetic effects are also explicitly introduced. This is the case of *ab initio* kinetic Monte Carlo, but this and connected materials science topics go well beyond the scope of this chapter.

10 The Future

On one side the future of DFT-based theoretical material science is in the improvement of the approximated xc functionals. On the other side, multiscale procedures for the extrapolation of atomistic information (energy as function of atomic configuration) should be developed further in order to describe equilibrium but also non-equilibrium conditions (time multiscale), but also long-range inhomogeneities of the considered material (space multiscale) in a reactive and possibly evolving environment (i.e., for

treating corrosion, chemical reactors, Earth-atmosphere chemistry and thermodynamics ...). It must be underlined that an accurate description at the electronic structure (atomistic) level is of fundamental importance as a basis of any multiscale extrapolation. In fact, in some fortunate cases statistical mechanics may “average out” inaccuracies at the atomistic level, but in other cases (that may be the majority) the upscaling may multiply the effect of such inaccuracies, especially if uncontrolled.

References

1. P. Hohenberg and W. Kohn, *Phys. Rev.* 136, B864 (1964)
2. M. Levy, *Phys. Rev. A* 26, 1200 (1982)
3. E. H. Lieb, *Rev. Mod. Phys.* 53, 603 (1981)
4. W. Kohn and L. J. Sham, *Phys. Rev.* 140, A1133 (1965)
5. E. P. Wigner *Trans. Faraday Soc.* 34, 678 (1938)
6. D. M. Ceperley and B. J. Alder *Phys. Rev. Lett.* 45, 566 (1980)
7. W. Kohn, *Reviews of Modern Physics* 71, 1253 (1999)
8. K. Burke, *J. Chem. Phys.* 136, 150901 (2012)
9. J. P. Perdew, *Phys. Rev. B* 33, 8822 (1986); 34, 7406(E) (1986)
10. J. P. Perdew, K. Burke, and M. Ernzerhof, *Phys. Rev. Lett.* 77, 3865 (1996); 78, 1396(E) (1997)
11. Y. Zhang, W. Yang, *Phys. Rev. Lett.* 80, 890 (1998)
12. M. Giantomassi, M. Stankovski, R. Shaltaf, M. Gruning, F. Bruneval, P. Rinke, and G.-M. Rignanese, *Physica Status Solidi B* 248, 275 (2011)
13. J. P. Perdew, R. G. Parr, M. Levy, and J. L. Balduz, *Phys. Rev. Lett.* 49, 1691 (1982)
14. J. P. Perdew, in *Density Functional Methods in Physics*, edited by R. M. Dreizler and J. da Providencia (Plenum, 1985), pp. 265308
15. M. Gruning, A. Marini, and A. Rubio, *J. Chem. Phys.* 124, 154108 (2006)
16. R. J. Bartlett and M. Musiał *Rev. Mod. Phys.* 79, 291 (2007)
17. L. A. Curtiss, K. Raghavachari, G. W. Trucks, J. A. Pople, *J. Chem. Phys.* 94, 7221 (1991)
18. A. Karton, A. Tarnopolsky, J. Lamère, and J. M. L. Martin, *J. Phys. Chem. A* 112, 12868 (2008)
19. P. Jurečka, J. Šponer, J. Černý, P. Hobza, *Phys. Chem. Chem. Phys.* 8, 1985 (2006)
20. Jan Řezáč, K. E. Riley, and P. Hobza *J. Chem. Theory Comput.* 7, 2427 (2011)
21. Y. Zhao, B. J. Lynch, D. G. Truhlar, *J. Phys. Chem. A* 108, 2715 (2004)
22. Y. Zhao, N. Gonzalez-Garca, D. G. Truhlar, *J. Phys. Chem. A* 109, 2012 (2005)
23. L. Goerigk, and S. Grimme, *Phys. Chem. Chem. Phys.* 13, 6670 (2011)
24. A. D. Becke, *J. Chem. Phys.* 98, 5648 (1993)
25. C. Lee, W. Yang, and R. G. Parr, *Phys. Rev. B* 37, 785 (1988)
26. A. Seidl, A. Grüning, P. Vogl, J. A. Majewski, and M. Levy, *Phys. Rev. B* 53, 3764 (1996)
27. J. Heyd, G. E. Scuseria, and M. Ernzerhof, *J. Chem. Phys.* 118, 8207 (2003); J. Heyd and G. E. Scuseria, *J. Chem. Phys.* 121, 1187 (2004)
28. A. Savin, *Recent Developments and Applications of Modern Density Functional Theory* (Elsevier, B. V., 1996), pp. 327357
29. E. N. Brothers, A. F. Izmaylov, J. O. Normand, V. Barone, and G. E. Scuseria, *J. Chem. Phys.* 129, 011102 (2008)
30. M. Jain, J. R. Chelikowsky, and S. G. Louie, *Phys. Rev. Lett.* 107, 216806 (2011)
31. D. Bohm, D. Pines, *Phys. Rev.* 92, 609 (1953)
32. J. Harl, L. Schimka, G. Kresse, *Phys. Rev. B* 81, 115126 (2010)
33. S. Grimme, *J. Comput. Chem.* 27, 1787 (2006)
34. G. Heimel, L. Romaner, J.-L. Bredas, E. Zojer, *Phys. Rev. Lett.* 96, 196806 (2006).
35. J. J. Rehr, E. Zaremba, and W. Kohn *Phys. Rev. B* 12, 2062 (1975)
36. D. Bohm, D. Pines, *Phys. Rev.* 92, 609 (1953).

37. D. C. Langreth, J. P. Perdew, *Phys. Rev. B* **15**, 2884 (1977).
38. J. F. Dobson, in *Topics in Condensed Matter Physics* (Ed. M. P. Das) 1994, Ch. 7 (Nova: New York)
39. L. Hedin, S. Lundqvist (1969) In: *Solid state physics: advances in research and applications*, vol 23. Academic Press, New York and London, p 1
40. K. S. Singwi, M. P. Tosi, R. H. Land, A. Sjolander, *Phys Rev* **176**, 589 (1968)
41. X. Ren, P. Rinke, C. Joas, and M. Scheffler, *J. Mater. Sci.* **47**, 7447 (2012).
42. X. Ren, A. Tkatchenko, P. Rinke, M. Scheffler, *Phys. Rev. Lett.* **106**, 153003 (2011)
43. J. Paier, X. Ren, P. Rinke, G. E. Scuseria, A. Gruneis, G. Kresse, M. Scheffler, *New J. Phys.* **14**, 043002 (2012)
44. A. Tkatchenko, M. Scheffler, *Phys. Rev. Lett.* **102**, 073005 (2009)
45. Y. Andersson, D.C. Langreth, B.I. Lundqvist, *Phys. Rev. Lett.* **76**, 102 (1996).
46. M. Dion, H. Rydberg, E. Schrder, D. C. Langreth, B. I. Lundqvist, *Phys. Rev. Lett.* **92**, 246401 (2004).
47. D. C. Langreth, B. I. Lundqvist, S. D. Chakarova-Kck, V. R. Cooper, M. Dion, P. Hyltdgaard, A. Kelkkanen, J. Kleis, L. Kong, S. Li, P. G. Moses, E. Murray, A. Puzder, H. Rydberg, E. Schrder, and T. Thonhauser, *J. Phys. Condens. Matter* **21**, 084203 (2009).
48. G. Roman-Perez, J. Soler, *Phys. Rev. Lett.* **103**, 096102 (2009)
49. A. Tkatchenko, L. Romaner, O.T. Hofmann, E. Zojer, C. Ambrosch-Draxl, and M. Scheffler, *MRS Bulletin* **35**, 435-442 (2010).
50. O. A. Vydrov, T. Van Voorhis, *Phys. Rev. Lett.* **103**, 063004 (2009).
51. J. Klimes, D. R. Bowler, A. Michaelides, *J. Phys. Condens. Matter* **22**, 022201 (2010).
52. A. Tkatchenko, R. A. DiStasio, Jr., R. Car and M. Scheffler, *Phys. Rev. Lett.* **108**, 236402 (2012)
53. R. A. DiStasio Jr., O. A. von Lilienfeld and A. Tkatchenko, *Proc. Natl. Acad. Sci. USA* **109**, 14791 (2012)
54. G.-X. Zhang, A. Tkatchenko, J. Paier, H. Appel and M. Scheffler, *Phys. Rev. Lett.* **107**, 245501 (2011)
55. V. G. Ruiz, W. Liu, E. Zojer, M. Scheffler and A. Tkatchenko, *Phys. Rev. Lett.* **108**, 146103 (2012)
56. R.A. DiStasio, Jr., V.V. Gobre, and A. Tkatchenko, *Psi-k Highlight of December 2012*.
57. K. Lee, E. D. Murray, L. Kong, B. I. Lundqvist, and D. C. Langreth, *Phys. Rev. B* **92**, 081101 (2010)
58. J. P. Perdew, M. Ernzerhof, and K. Burke, *J. Chem. Phys.* **105**, 9982 (1996).
59. Y. Zhao and D. G. Truhlar, *Chem. Phys. Lett.* **502**, 1 (2011)
60. J. E. Moussa, P. A. Schultz, and J. R. Chelikowsky, *J. Chem. Phys.* **136**, 204117 (2012)
61. A. V. Krukau, O. A. Vydrov, A. F. Izmaylov, and G. E. Scuseria, *J. Chem. Phys.* **125**, 224106 (2006)
62. P. Ehrenfest, *Z. Phys. A* **45**, 455 (1927)
63. P. A. M. Dirac, *Proc. Camb. Phil. Soc.* **26**, 376 (1930)
64. R. Car and M. Parrinello, *Phys. Rev. Lett.* **55**, 2471 (1985)
65. H. C. Andersen, *J. Chem. Phys.* **72**, 2384 (1980)
66. Parrinello M., Rahman A., *Phys Rev Lett* **45**, 1196 (1980)
67. G. Galli, R. M. Martin, R. Car, and M. Parrinello *Phys. Rev. Lett.* **63**, 988 (1989)
68. R. Iftimie and M. E. Tuckerman, *J. Chem. Phys.* **122**, 214508 (2005)
69. D. Sebastiani and M. Parrinello, *J Phys Chem A* **105**, 1951 (2001)
70. B. Grabowski, L. Ismer, T. Hickel, and J. Neugebauer, *Phys Rev B* **79**, 134106 (2009)
71. D. Hohl and R. O. Jones , *Phys. Rev. B* **50**, 17047 (1994)
72. T. Morishita, *Phys. Rev. Lett.* **87**, 105701 (2001)
73. L. M. Ghiringhelli and E. J. Meijer, *J. Chem. Phys.* **122**, 184510 (2005)
74. D. Marx, M. E. Tuckerman, J. Hutter, M. Parrinello, *Nature* **397**, 601 (1999)
75. D. Marx and J. Hutter, in "Modern Methods and Algorithms of Quantum Chemistry", J. Gro-tendorst (Ed.), John von Neumann Institute for Computing, Jülich, NIC Series, Vol. 1, 301 (2000.)
76. B. Kirchner, P. J. di Dio, and J. Hutter, *Top. Curr. Chem.* **307**, 109 (2012)
77. P. L. Silvestrelli, M. Parrinello *Phys. Rev. Lett.* **82**, 3308 (1999)

78. J. VandeVondele, F. Mohamed, M. Krack, J. Hutter, M. Sprik, M. Parrinello *J. Chem. Phys.* **122**, 014515 (2005)
79. M. Bühl, A. Chaumont, R. Schurhammer, G. Wipff, *J. Phys. Chem. B* **109**, 18591 (2005)
80. K. Laasonen, M. L. Klein, *J. Am. Chem. Soc.* **116**, 11620 (1994)
81. C. Krekeler, L. Delle Site, *J. Phys.: Condens. Matter* **19**, 192101 (2007)
82. M. Pagliai, S. Raugai, G. Cardini, V. Schettino *J. Mol. Struct. (Theochem)* **630**, 141 (2003)
83. J. Blumberger, Y. Tateyama, M. Sprik, *Comput. Phys. Commun.* **169**, 256 (2005)
84. G. Bussi, D. Donadio, and M. Parrinello, *J. Chem. Phys.* **126**, 014101 (2007)
85. M. Ceriotti, G. Bussi, M. Parrinello, *J. Chem. Theory Comput.* **6**, 1170 (2010)
<http://gle4md.berlios.de/>
86. M. De Koning, A. Antonelli, and S. Yip. *Phys. Rev. Lett.* **83**, 3973 (1999)
87. A. Laio and M. Parrinello, *Proc. Natl. Acad. Sci.* **99**, 12562 (2002)
88. R. Martoňák, A. Laio, and M. Parrinello, *Phys. Rev. Lett.* **90**, 075503 (2003)
89. X. Wang, S. Scandolo, and R. Car, *Phys. Rev. Lett.* **95**, 185701 (2005)
90. D. Donadio, L. Spanu, I. Duchemin, F. Gygi, and G. Galli, *Phys. Rev. B* **82**, 020102(R) (2010)
91. R. Martonak, D. Donadio, A.R. Oganov, and M. Parrinello, *Nat. Mater.* **5**, 623 (2006)
92. M. Rossi, V. Blum, P. Kupser, G. von Helden, F. Bierau, K. Pagel, G. Meijer, and M. Scheffler, *J. Phys. Chem. Lett.* **1**, 3465-3470 (2010).
93. A. Tkatchenko, M. Rossi V. Blum, J. Ireta, and M. Scheffler, *Phys. Rev. Lett.* **106**, 118102 (2011).
94. L. M. Ghiringhelli, P. Gruene, J. T. Lyon, D. M. Rayner, G. Meijer, André Fielicke, and M. Scheffler, accepted to *New J. Phys.* (2013)
95. C. Stampfl, M. V. Ganduglia-Pirovano, K. Reuter M. Scheffler, *Surf. Sci.* **500**, 368-394 (2002).
96. K. Reuter and M. Scheffler, *Phys. Rev. B*, **65**, 035406 (2001)
97. K. Reuter and M. Scheffler, *Phys. Rev. B*, **68**, 045407 (2003)
98. E.C. Beret, L.M. Ghiringhelli and M. Scheffler, *Faraday Discuss.* **152**, 153 (2011).
99. E. C. Beret, M. M. van Wijk, L. M. Ghiringhelli. *Int. J. Quantum Chem.* (2013).
DOI: 10.1002/qua.24503.
100. S. Bhattacharya, S. Levchenko, L.M. Ghiringhelli and M. Scheffler. Accepted to *Phys. Rev. Lett.* (2013).
101. C. M. Weinart and M. Scheffler, *Defects in Semiconductors*, *Mat. Sci. Forum* **1012**, (1986)
102. M. Scheffler and J. Dabrowski, *Philos. Mag. A* **58**, 107 (1988)
103. N.A. Richter, S. Socolo, S.V. Levchenko, J. Sauer, and M. Scheffler, *Phys. Rev. Lett.* **111**, 045502 (2013).
104. S.-H. Lee, W. Moritz, and M. Scheffler, *Phys. Rev. Lett.* **85**, 3890 (2000)